

## The effect of deposition process exchange current density on the thin metal film formation on inert substrate

K. I. POPOV,<sup>1</sup> B. N. GRGUR,<sup>1</sup> E. R. STOJILKOVIĆ,<sup>2</sup> M. G. PAVLOVIĆ<sup>3</sup> and N. D. NIKOLIĆ<sup>3</sup>

<sup>1</sup>Faculty of Technology and Metallurgy, Karnegijeva 4, P. O. Box 494, Belgrade, <sup>2</sup>Faculty of Agriculture, Zemun, Belgrade, and <sup>3</sup>ICTM-Institute of Electrochemistry, Njegoševa 12, Belgrade, Yugoslavia

(Received 27 June 1996, revised 14 February 1997)

The initial stage of thin surface metal film formation on inert substrate is considered. The simultaneous action of both active centers and nucleation exclusion zones was taken into consideration when discussing the saturation nucleus density. The saturation nucleus density increases with increasing number of active centers and decreasing the radii of nucleation exclusion zones (enhancing the thin metal film formation). At one at the same deposition current density deposition overpotential increases with decreasing deposition process exchange current density, leading to the increase in the number of active centers and to decrease of crystallization overpotential and radii of nucleation exclusion zones. Because of this compact surface metal film will be formed at a lower quantity of electrodeposited metal with a decrease in exchange current density.

*Key words:* metal electrodeposition, surface metal film formation, thin metal film formation.

Metal electrodeposition on inert electrodes begins by the formation of separate centers growth until a continuous or disperse deposit is produced. Although the kinetics of electrolytic nucleation and subsequent growth have been the subject of extensive studies, little attention has been given to the screening action of the growing nuclei. The nature of this phenomenon should be made clear by the following arguments: once a nucleus of the depositing metal is formed, the flowing current causes a local deformation of the electric field in the vicinity of the growing center. As a result, an ohmic potential drop occurs along the nucleus-anode direction. Considering the high dependence of the nucleation rate on the overpotential, new nuclei should be expected to form only outside the spatial region around the initial nucleus where their potential difference between the cathode and the electrolyte surpasses some critical value  $\eta_c$ . Using simple mathematics one obtains for the radius of the screening zone in the ohmic-controlled deposition:

$$r = f \frac{E}{E - \eta_c} \rho \quad (1)$$

where  $\eta_c$  is the critical overpotential for nucleation to occur,  $E$  is the ohmic drop between anode and cathode,  $f$  is the numerical factor and  $\rho$  is the radius of the nucleus. The radius of the screening zone depends on the  $E$  and  $\eta_c$  values. At constant  $\eta_c$  an increase in  $E$  leads to a decrease in the radius of the screening zone; the same appears if  $\eta_c$  decreases at constant  $E$ .<sup>1</sup>

During the cathodic process at low  $j/j_0$  the crystallization overpotential is considerably high; with increasing  $j/j_0$  however, it rapidly decrease.<sup>2</sup> Hence, for  $j_0 \rightarrow 0$ ,  $r \rightarrow 0$ .

It has been established experimentally that the number of nuclei deposited electrolytically onto inert electrodes increases linearly with time after a period of induction. After a sufficient length of time it reaches a saturated value that is independent of time. The saturation value's density increases with the overpotential applied and is strongly dependent on the concentration of the electrolyte and the state of the electrode surface.<sup>3-5</sup>

Kaischew and Mutaftchiew<sup>6</sup> explained the phenomenon of saturation on the basis of energetic inhomogeneity of the substrate surface. They assumed that the active centers have different activity, or different critical overpotential, with respect to formation of the nuclei. Nuclei can be formed on those centers whose critical overpotential is lower than or equal to that applied to the electrolytic cell from the outside. The higher the overpotential applied, the greater the number of weaker active sites taking part in the nucleation process and hence the greater saturation nucleus density. The formation and growth of nuclei is necessarily followed by the formation and growth of nucleation exclusion zones. After some time the zones overlap to cover the substrate surface exposed for nucleation, thus terminating the nucleation process.

The simultaneous action of both active centers and nucleation exclusion zones must be taken into consideration when discussing the dependence of the number of nuclei on time. In the limiting case for active centers, when screening zones are not formed, the saturation nucleus density is exactly equal to the integral number of active centers. In the limiting case for nucleation exclusion zones the saturation nucleus density is directly proportional to the nucleation rate and reversely to the zone growth rate.<sup>5</sup> It is obvious that saturation nucleus density is larger in the first than in the second case, because of the deactivation of active centers by the overlapping nucleation exclusion zones.

The classical expression for the steady state nucleation rate  $J$  is given by:<sup>7-9</sup>

$$J = K_1 \exp\left(-\frac{K_2}{\eta^2}\right) \quad (2)$$

where  $K_1$  and  $K_2$  are practically overpotential-independent constants. The equation is valid for a number of systems regardless of the exchange current density value for the deposition process.<sup>10-14</sup> At one and the same deposition current density,  $j$  decreasing  $j_0$  leads to an increasing nucleation rate and a decrease in the radii of the nucleation exclusion zones. Hence, for  $j/j_0 \rightarrow 0$  the limiting case for nucleation exclusion zones can be expected, and for  $j/j_0 \rightarrow \infty$  the limiting case for active centers.

The saturation nucleus density, *i.e.*, the deposition process exchange current density, strongly affects the morphology of metal deposits. At high exchange current densities the radii of screening zones are larger and saturation nucleus density is low. This permits the formation of large, well-defined crystal grains and granular deposit growth. At low exchange current densities the screening zones' radii are low, or equal to zero, the nucleation rate is large and thin surface film can be easily formed.

Nucleation does not occur simultaneously over all the cathode surface but is a process extended in time so that crystals generated earlier may be considerably larger in size than later generated ones. This causes periodicity in the surface structure of polycrystalline electrolytic deposits, as well as coarseness of the thin metal film formed even on ideally smooth substrate. Hence, the larger the nucleation rate, the more homogeneous the distribu-

tion of crystal grain size which leads to a smoother deposit. Obviously, periodicity in the surface structure is a more complicated problem, as shown by Kovarskii and Lisov,<sup>15</sup> but for the purpose of this article the above conclusion is sufficient. The purpose of this work is to confirm the basic facts of the above theories and to show the effect of exchange current density on the deposition process of thin metal film formation on inert substrate.

#### EXPERIMENTAL

Silver was deposited on platinum plane electrode, nickel and cadmium on copper stationary wire electrode and copper on silver stationary wire electrode. Potentiostatic polarization measurements and galvanostatic deposition were performed in the open cells at room temperature. The counter and reference electrodes were of pure corresponding metal. The solutions used were: 0.1 M AgNO<sub>3</sub> + 0.5 M HNO<sub>3</sub>; 0.1 M AgNO<sub>3</sub> + 0.5 M (NH<sub>4</sub>)<sub>2</sub>SO<sub>4</sub> solution to which was added ammonium hydroxide to dissolve the silver precipitate; 0.07 M CuSO<sub>4</sub> + 0.5 M H<sub>2</sub>SO<sub>4</sub>; 0.07 M NiSO<sub>4</sub> + 0.5 M Na<sub>2</sub>SO<sub>4</sub> + 30 g/l H<sub>3</sub>BO<sub>3</sub>, pH = 4, and 0.07 M CdSO<sub>4</sub> + 0.5 M H<sub>2</sub>SO<sub>4</sub> made of p.a. chemicals and doubly distilled water.

Exchange current densities for copper and nickel deposition processes were obtained by extrapolating the Tafel line to the zero overpotential, and for cadmium from the slope of the overpotential-current density dependence in the linear polarization experiments ( $\pm 10$  mV around zero overpotential). The morphology of the metal deposits was investigated by means of scanning electron microscopy (SEM), using a JOEL T20 microscope.

#### RESULTS AND DISCUSSION

It was shown<sup>16</sup> that silver deposition from the nitrate bath is characterized by  $j_0 \gg j_L$ , while from the ammonium complex salt bath there is a well-defined region in which the deposition process is under pure activation control ( $b_k = 60$  mV dec<sup>-1</sup>,  $j_0 = 0.25$  mA cm<sup>-2</sup>,  $j_L = 8$  mA cm<sup>-2</sup>,  $j_0 < j_L$ ).

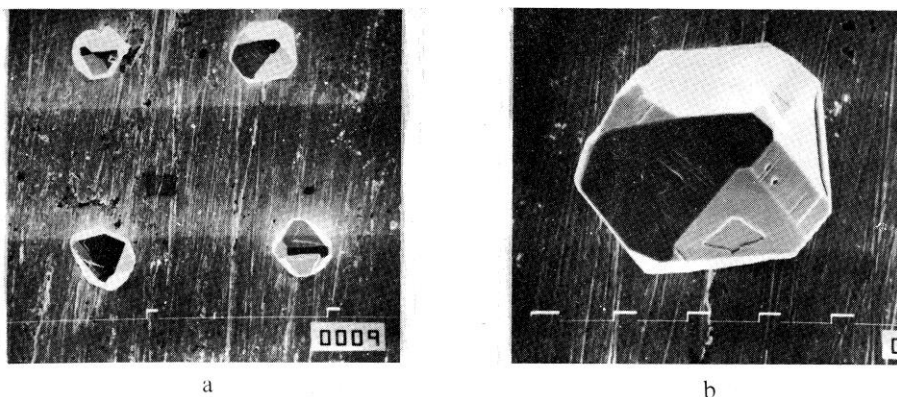


Fig. 1. Silver deposit on the platinum plane electrode from 0.1 M AgNO<sub>3</sub> in 0.5 M HNO<sub>3</sub> at room temperature. Deposition overpotential 6 mV. Deposition time 45 min. Magnification: a)  $\times 500$ ; b)  $\times 2000$ .

The silver grains obtained from the nitrate solution on the platinum substrate are presented in Fig. 1. In Fig. 2 silver deposit from nitrate bath on the substrate obtained as this from Fig. 1 and in Fig. 3 silver deposit from ammonium complex bath on the substrate obtained as this from Fig. 2 are shown. It is seen from Fig. 2 that a large nucleation exclusion zones are formed around initial grains during deposition from nitrate bath. It is to note that the same situation as in this case appears in deposition of silver from nitrate solution on the glassy carbon electrode,<sup>17</sup> meaning that exclusion zones formation do not depend on the

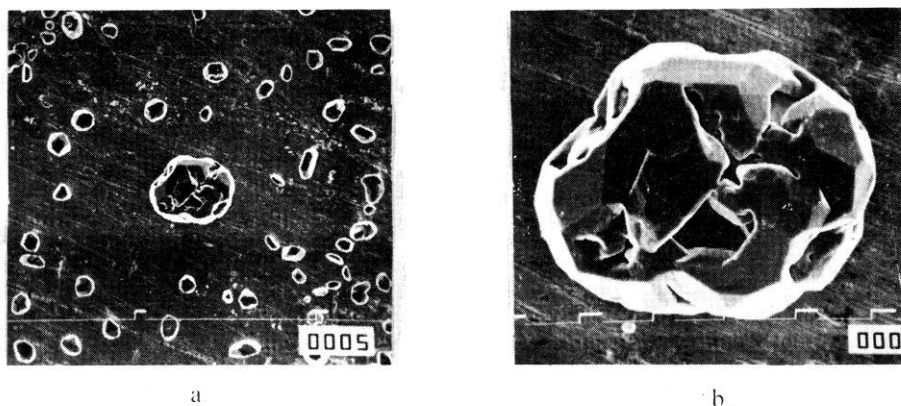


Fig. 2. Silver deposit on the substrate formed as this from Fig. 1, from the same electrolyte. Current density  $2.9 \text{ mA/cm}^2$ . Deposition time 2 min. Magnification: a)  $\times 500$ ; b)  $\times 2000$ .

substrate. They practically do not exist in deposition from the ammonium complex bath. Besides, new nucleation is seen on the initial grain in Fig. 3. It seems that exchange current

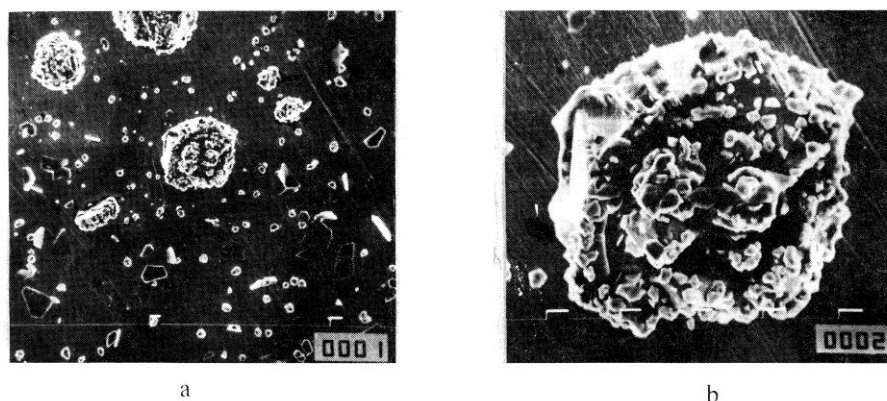


Fig. 3. Silver deposit on the substrate formed as this from Fig. 2 from  $0.1 \text{ M AgNO}_3$  in  $0.5 \text{ M (NH}_4)_2\text{SO}_4$  to which was added ammonium hydroxide to dissolve the silver precipitate. Current density  $2.9 \text{ mA/Cm}^2$ . Deposition time 1 min. Magnification: a)  $\times 500$ ; b)  $\times 2000$ .

density value for the deposition process on the same substrate can be used in the analysis of the surface film formation on an inert substrate. This fact requires further investigations.

TABLE I. The exchange current density, and  $j_L/j_o$  ratios for Cd, Cu and Ni deposition processes

Metal	$j_o/\text{A cm}^{-2}$	$j_L/j_o$
Cadmium	$1.5 \times 10^{-3}$	3.0
Copper	$3.2 \times 10^{-4}$	14.4
Nickel	$1.6 \times 10^{-9}$	$2.9 \times 10^6$

The polarization curves for nickel, copper and cadmium deposition, corresponding

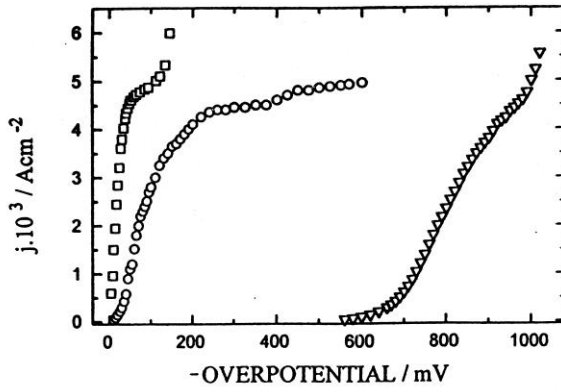


Fig. 4. Polarization curve for (□), cadmium, (O) copper and (Δ) nickel depositions.

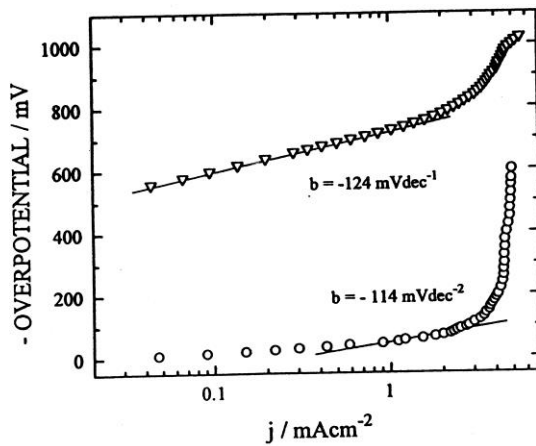


Fig. 5. Tafel plots of (O) copper and (Δ) nickel depositions.

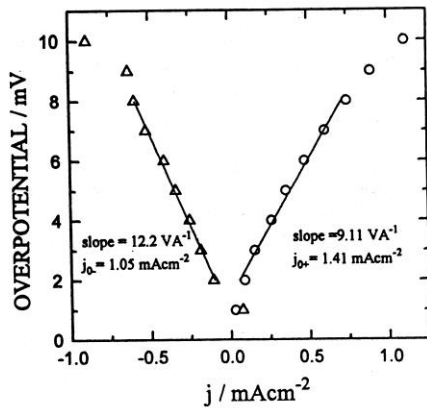


Fig. 6. Linear overpotential-current density dependence of the cadmium deposition-dissolution process.

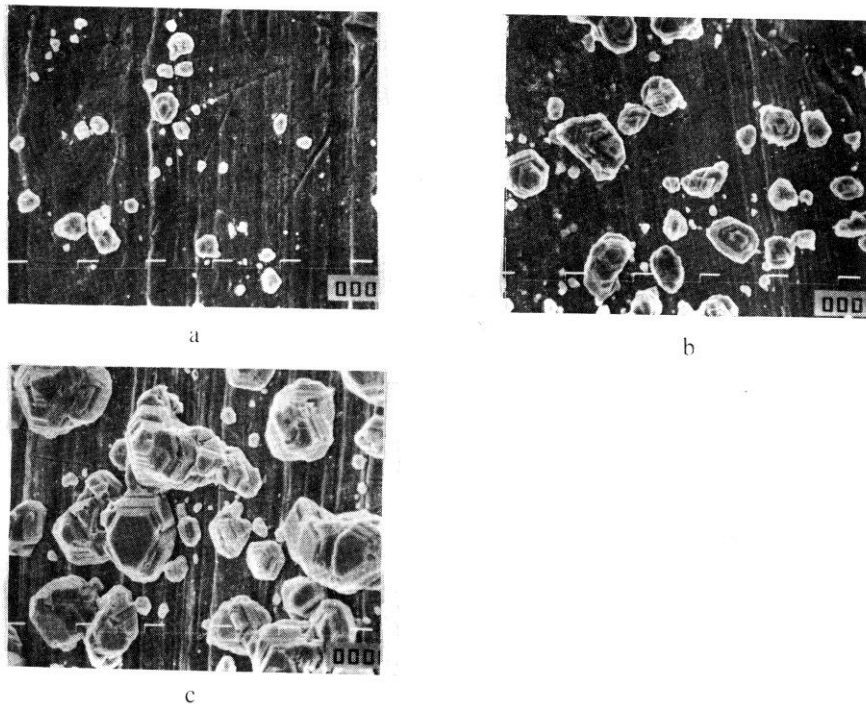


Fig. 7. SEM microphotograph of cadmium deposits on copper substrate obtained at current density of  $1 \text{ mA cm}^{-2}$ . Deposition time: a)  $t = 120 \text{ s}$ , b)  $t = 300 \text{ s}$ , c)  $t = 1200 \text{ s}$ . Magnification  $\times 2000$ .

Tafel plots and the results of linear polarization experiments are shown in Figs. 4, 5 and 6, respectively. The limiting diffusion currents in all cases are practically the same, but exchange current densities (given in Table I) are very different. Hence, the  $j_L/j_0$  ratio, Table I, which determines the morphology of electrodeposited metal<sup>18</sup> depends only on the exchange current density values.

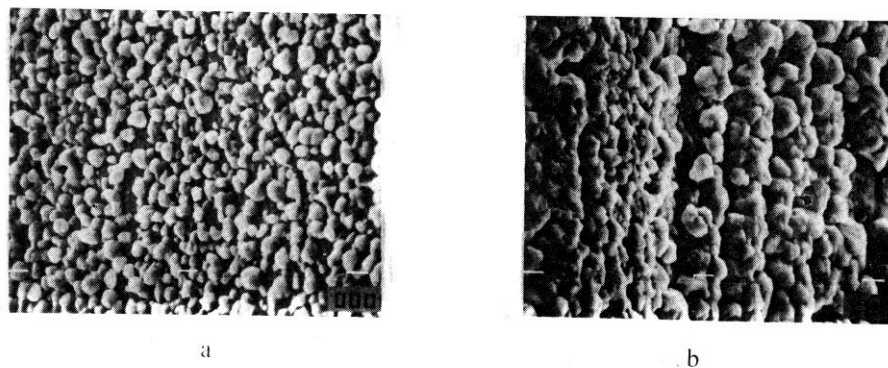


Fig. 8. SEM microphotograph of copper deposits on silver substrate obtained at current density of  $1 \text{ mA cm}^{-2}$ . Deposition time: a)  $t = 300 \text{ s}$ , b)  $t = 1200 \text{ s}$ . Magnification  $\times 5000$ .

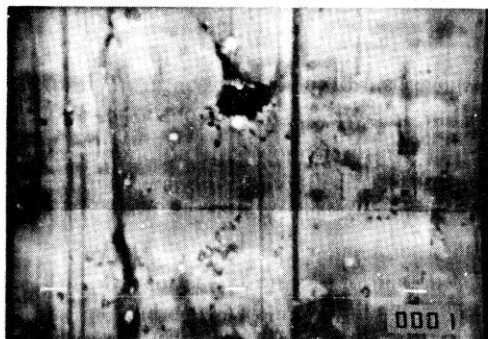


Fig. 9. SEM microphotograph of nickel deposits on copper substrate obtained at current density of  $1 \text{ mA cm}^{-2}$ . Deposition time:  $t = 120 \text{ s}$ . Magnification  $\times 5000$ .

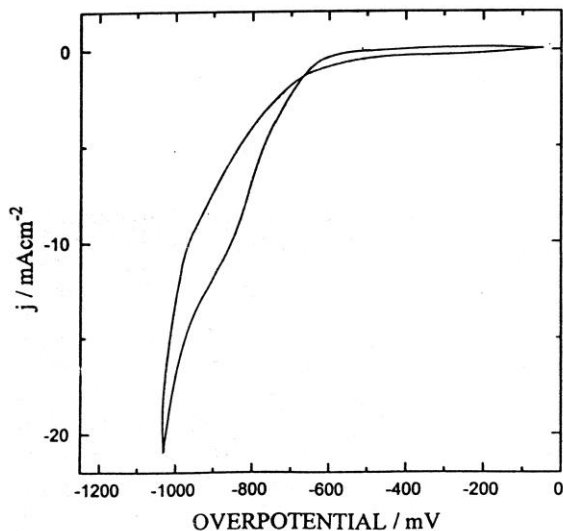


Fig. 10. Cyclic voltammogram of cadmium deposition at Cd electrode,  $v = 100 \text{ mV s}^{-1}$ .

Electrodeposits of cadmium, copper and nickel are shown in Figs. 7, 8 and 9, respectively. In the cadmium deposition, boulders are formed by the independent growth of formed nuclei inside zones of zero nucleation. Because of the high  $j_0$  value the deposition overpotential is lower and the crystallization overpotential is relatively large and the screening zone, according to Eq. 1, is relatively large. On the other hand, the nucleation rate is low. This results in deposits shown in Fig. 7.

In the case of copper, the surface film is practically formed at the same or lower quantity of electricity, as seen from Fig. 8, due to the lower exchange current density.

The value of the deposition overpotential is larger than in the case of cadmium and the crystallization overpotential is lower, resulting in a decrease in the zero nucleation zone radius, and the nucleation rate is also considerably larger. A further decrease in the exchange current density value, as in the case of Ni, leads to the situation shown in Fig. 9. A surface film is formed, but is a porous one, probably due to the hydrogen co-deposition. It can be seen from Fig. 4 that the limiting diffusion current density plateaus are not parallel to the

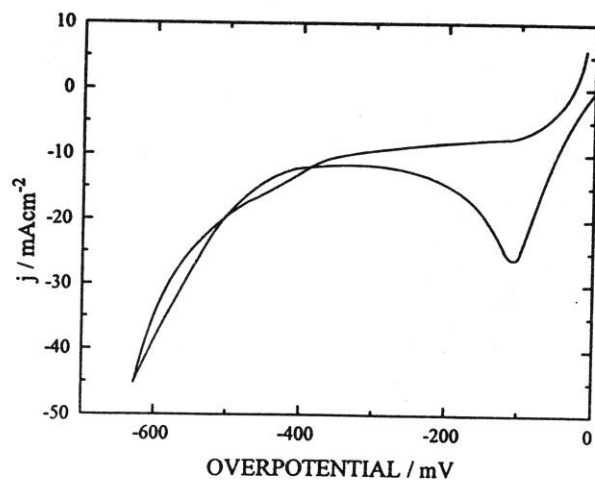
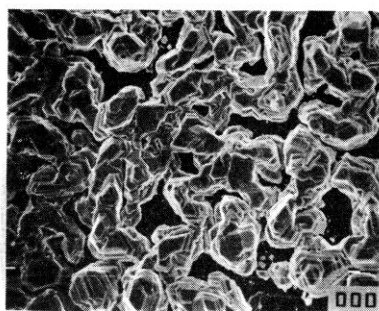
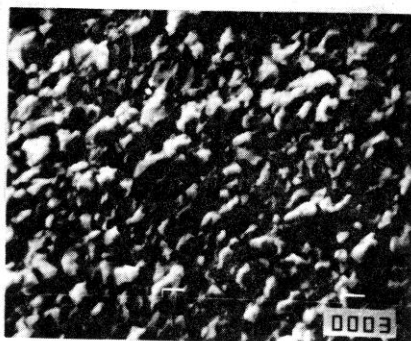


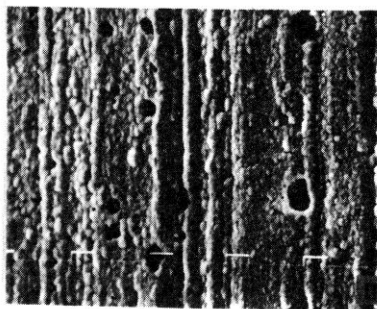
Fig. 11. Cyclic voltammogram of nickel deposition at Ni electrode,  $\nu = 100 \text{ mV s}^{-1}$ .



a



b



c

Fig. 12. SEM microphotograph of metal deposits at current density of  $3.5 \text{ mA cm}^{-2}$  for  $t = 1800 \text{ s}$ : a) cadmium, magnification  $\times 1000$ , b) copper, magnification  $\times 2000$  and c) nickel, magnification  $\times 2000$ .

x-axis for cadmium and nickel depositions. It can be seen from Figs. 4 and 10 that in cadmium deposition hydrogen evolution does not take place at deposition overpotential and the slope



of the plateau is probably due to the fast increase in electrode surface coarseness and dendritic growth. In the case of nickel the hydrogen co-deposition can take place even at low deposition current densities, Figs. 4 and 11.

Cadmium surface film is not formed even at larger deposition current densities and quantity of electrodeposited metal, as seen from Fig. 12.

At the same time the copper surface film deposited under the same conditions is completely formed and the amplification of surface coarseness takes place. In the case of nickel surface, film is also formed as expected, but it is less coarse and porous.

Hence, a decrease in the exchange current density value of the deposition process enhances the thin surface metal film formation on inert substrate due to the increase in the nucleation rate and decrease in the radius of the zero nucleation zones. Because of this, compact surface metal film is formed at a lower quantity of electrodeposited metal, and its roughness and porousness decrease with a decrease in exchange current density. On the other hand, at sufficiently negative equilibrium potentials and low hydrogen overvoltage for an inert substrate, a decrease in exchange current density of the deposition process can produce a porous deposit due to hydrogen codeposition.

## ИЗВОД

## УТИЦАЈ ГУСТИНЕ СТРУЈЕ ИЗМЕНЕ НА ПРОЦЕС ТАЛОЖЕЊА ТАНКИХ ФИЛМОВА МЕТАЛА НА НЕСРОДНИМ ПОДЛОГАМА

К. И. ПОПОВ,<sup>1</sup> Б. Н. ГРУР,<sup>1</sup> Е. Р. СТОЈИЛКОВИЋ,<sup>2</sup> М. Г. ПАВЛОВИЋ<sup>1</sup> и Н. Д. НИКОЛИЋ<sup>3</sup>

<sup>1</sup>Технолошко-металуршки факултет, Универзитет у Београду, Карнегијева 4, п. пр. 494, Београд, <sup>2</sup>Пољопривредни факултет, Земун - Београд, <sup>3</sup>ИХТМ-Центар за електростројарију, Њеђинска 12, Београд

Разматрана је почетна фаза настајања површинског филма метала. Дискутован је утицај активних центара и зона искључења нуклеације на засићену густину нуклеуса. Засићена густина нуклеуса расте са порастом броја активних центара и са смањењем полупречника зона искључења нуклеације, што стимулише настајање танког филма метала. При једној густини струје таложња пренапетост расте са смањењем густине струје измене за процес таложња, што доводи до повећавања броја активних центара и смањења кристализационе пренапетости и полупречника зона искључења. На тај начин се формирају компактни површински филмови при таложњу мање количине метала када је процес таложња окарактерисан мањом вредношћу густине струје измене.

(Примљено 27. јуна 1996, ревидирано 14. фебруара 1997)

## REFERENCES

1. I. Markov, A. Boynov, S. Toshev, *Electrochim. Acta* **18** (1973) 377
2. V. Klapka, *Collection Czechoslov. Chem. Commun.* **35** (1970) 899
3. S. Toshev, I. Markov, *Ber. Bunsenges. Phys. Chem.* **73** (1969) 184
4. A. Scheludko, M. Todorova, *Comn. Bulg. Acad. Sci. (Phys.)* **3** (1952) 61
5. I. Markov, *Thin Solid Films* **35** (1976) 11
6. R. Kaischew, B. Mutaftschiew, *Electrochim. Acta* **10** (1965) 643
7. R. Becker, W. Doring, *Ann. Phys. (Leipzig)* **24** (1935) 719
8. G. Tohmfor, M. Volmer, *Ann. Phys. (Leipzig)* **B33** (1938) 109
9. T. Erdy-Gruz, M. Volmer, *Z. Phys. Chem.* **157A** (1931) 165
10. R. Kaischew, B. Mutaftschiew, *Z. Phys. Chem.* **204** (1955) 334
11. B. Mutaftschiew, R. Kaischew, *Izv. BAN* **5** (1955) 77
12. R. Kaischew, I. Gutzow, *Electrochim. Acta* **9** (1964) 1047

13. A. Scheludko, G. Bliznakov, *Izv. BAN* **2** (1951) 227
14. I. Gutzow, *Izv. Inst. Fiz. Chim. Bulgar. Acad. Nauk.* **4** (1964) 69
15. N. Y. Kovarskii, A. V. Lisov, *Elektrokhimiya* **20** (1984) 221
16. K. I. Popov, N. V. Krstajić, S. R. Popov, *Surf. Technol.* **20** (1983) 203
17. G. Adžić, *Ph. D. Thesis*, University of Belgrade, 1992
18. K. I. Popov, N. V. Krstajić, *J. Appl. Electrochem.* **13** (1985) 775.

